The Survival of Ice Particles Falling from Cirrus Clouds in Subsaturated Air

W. D. HALL AND H. R. PRUPPACHER

Department of Meteorology, University of California, Los Angeles 90024

(Manuscript received 28 April 1976, in revised form 2 July 1976)

ABSTRACT

A theoretical study has been carried out to determine the relevant microphysical processes which control the survival distance of ice particles falling from cirrus clouds in subsaturated air, and to determine the atmospheric conditions which are necessary for such particles to "seed" lower level supercooled clouds and thereby initiate glaciation. Differential equations were developed which describe the heat and mass transfer during the evaporation of cirrus ice particles. In these equations forced convection and kinetic effects were included. Spherical, columnar and plate-like ice particles were considered. The effect of radiative heat exchange between an ice particle and its environment was studied in terms of maximum and minimum physical limits for the upward and downward radiation fluxes. Using these limits and the known emission and absorption properties of ice, we concluded that radiative heat transfer changes the survival distance of columnar ice crystals falling from cirrus clouds by less than 10% if the relative humidity of the environmental air is less than 70%. Considering the radiative effects and a wide range of values for the initial size and ice particle bulk density, and for the temperature and humidity conditions of the ambient air, the present theoretical model showed that ice particles could survive distances of up to 2 km when the relative humidity with respect to ice was below 70% in a typical mid-latitude atmosphere. Larger survival distances are only possible if the ambient air has relative humidities larger than 70%. The theoretical model is compared to several field observations on evaporating cirrus ice particles. Good agreement was found with observational data when the atmospheric temperature and humidity profiles were available for the site at which the ice particles were sampled.

1. Introduction

Although more than 30 years have passed since the first quantitative study on the ice particles in cirrus clouds were carried out *in situ* by Weickmann (1945, 1949), cloud physicists have paid astonishingly little attention to the characteristics of these clouds. Only rather recently have cirrus clouds received renewed attenion. In particular, there was interest in studying the effects of cirrus clouds on atmospheric heat balance and the effects of cirrus clouds on measuring the atmospheric temperature and moisture structure from orbiting meteorological satellites (Platt, 1975; Fleming and Cox, 1974; Liou, 1973; Hansen and Pollack, 1970; Kuhn and Weickmann, 1969; Valovcin, 1968). Microphysical studies in cirrus clouds have recently been carried out by Heymsfield (1973, 1975; Heymsfield and Knollenberg, 1972; Jiusto and Weickmann, 1973). These studies showed that cirrus ice particles, although present in rather low number concentrations, may be as large as 1–2 mm in size. It is obvious that such particles have considerable fallspeeds. One may therefore ask for the distance which such cirrus ice particles would survive once they have fallen out of the cloud, and, if they could survive considerable distances, whether they would "seed" lower level supercooled clouds and in this way provide a mechanism for initiation of cloud glaciation.

Braham and Spyers-Duran (1967) and Braham (1967) were the first to address themselves to this question. While flying beneath cirrus clouds they attempted to detect and document remnants of cirrus ice particles which they thought might exist some distance below the level of visible cirrus. Their observations indicated that cirrus ice particle trails with concentrations of 10^5 to 10^6 particles per cubic meter can survive a fall distance of over 5 km in clear air of relative humidities as low as 30% with respect to ice saturation. In an effort to explain their observations Braham and Spyers-Duran presented some crude calculations which involved solving a simplified form of the diffusional heat and mass transfer equations for individual ice particles with spherical and columnar shapes. From these calculations they concluded that the sizes required for ice spheres or columns to survive the observed 5 km fall under the given atmospheric conditions were too large to be compatible with the cirrus microphysical observations of Weickmann (1945, 1949).

In order to more quantitatively illucidate this problem, we studied the mass and heat transfer pro-

cesses of individual ice particles of different shapes and bulk densities at cirrus cloud levels in the atmosphere, and attempted to predict the distance which these ice particles would survive when penetrating ice-subsaturated air. In these computations we included forced convection and kinetic effects as well as effects due to heat exchange by radiation. A summary of this study is given below. A more detailed description is found in Hall (1976).

2. Theoretical framework

The evaporation process of an ice particle in air consists of simultaneous transfer of heat and mass. Transfer of these quantities is brought about by the diffusion of water vapor and heat through air to and from the particle. If the particle is sufficiently large the diffusion will be enhanced by forced convection which is a consequence of the particle's falling motion in the earth's gravitational field. If the particle is smaller than a critical size the diffusion is limited by kinetic processes. In addition to the transport of heat by molecular and convective diffusion, one needs to consider the radiative heat exchange between the ice particle and its environment.

The equation which we used for the mathematical and physical framework of this study represents a combination of relations formulated by various authors. While the basic set of equations for the diffusional growth of an ice crystal has been summarized by Mason (1971), more detailed equations for the diffusional growth for various shaped ice crystals were formulated by Koenig (1971) and by Jayaweera (1971). The effects of ventilation on the diffusional growth and evaporation of cloud particles have been discussed by Beard and Pruppacher (1971) and by Pitter *et al.* (1974). The kinetic effects on the diffusional growth mechanism have been studied by many workers, most notably by Fitzgerald (1974), Fukuta and Walter (1970), Fuchs (1959) and Schrage (1953).

Considering these previous studies we formulated the rate of mass change dm/dt of the ice particle as

$$\frac{dm}{dt}=4\pi C\mathfrak{D}F_\beta[\rho_{v,\infty}-\rho_{\mathrm{sat},i}(T_s)]f_m, \tag{1}$$

where

$$f_m=\bar{\mathrm{N}}_{\mathrm{Sh}}/(\bar{\mathrm{N}}_{\mathrm{Sh}})_0, \tag{2}$$

$$(\bar{\mathrm{N}}_{\mathrm{Sh}})_0=4\pi C/P, \tag{3}$$

$$F_\beta=\frac{r^*}{r^*+l_m^*}, \tag{4}$$

$$r^*=S/(4\pi C), \tag{5}$$

$$l_m^*=\left(\frac{2\pi M_w}{\mathfrak{R}T_s}\right)^{\frac{1}{2}}\frac{\mathfrak{D}f_m}{2\beta/(2-\beta)}. \tag{6}$$

The symbols in Eqs. (1)–(6) and all subsequent equations in this paper are defined in the Appendix.

The rate of heat exchange dQ/dt between the ice particle and its environment was formulated as

$$\frac{dQ}{dt}=4\pi CKF_\alpha(T_\infty-T_s)f_Q+S\Phi_R, \tag{7}$$

where

$$F_\alpha=\frac{r^*}{r^*+l_Q^*}, \tag{8}$$

$$l_Q^*=Kf_Q/(\rho_a\tfrac{1}{4}\bar{v}_r\alpha c_p), \tag{9}$$

$$f_Q=\bar{\mathrm{N}}_{\mathrm{Nu}}/(\bar{\mathrm{N}}_{\mathrm{Nu}})_0 \tag{10}$$

$$(\bar{\mathrm{N}}_{\mathrm{Nu}})_0=4\pi C/P. \tag{11}$$

Assuming that during evaporation the total amount of heat absorbed by the particle is proportional to the mass loss of the particle, Eqs. (1) and (7) are coupled by

$$\frac{dQ}{dt}=-\mathfrak{L}_s\frac{dm}{dt}. \tag{12}$$

3. Discussion of the pertinent physical parameters

Some of the physical parameters involved in Eqs. (1)–(12) can be considered well known and therefore need no further discussion. These are the thermal conductivity of moist air K (Beard and Pruppacher, 1971), the latent heat of sublimation $\mathfrak{L}_s$ [*Smithsonian Meteorological Tables* (SMT), 1968], the specific heat of moist air c_p (SMT), the saturation density of water vapor with respect to ice $\rho_{\mathrm{sat},i}(T)$ (SMT), and the density of moist air ρ_a (SMT).

Other physical parameters have been topics of considerable controversy over the past years and therefore need further discussion. These are the diffusivity $\mathfrak{D}$ of water vapor in air, the shape factor C affecting stationary diffusion to and from an arbitrary shaped ice particle, the ventilation factors f_m and f_Q for mass and heat diffusion, and the evaporation coefficient β and thermal accommodation coefficient α for ice. We shall briefly consider each of these in turn.

a. The diffusivity of water vapor in air

$\mathfrak{D}$ has been experimentally measured only for temperatures above 0°C. In this temperature range the experimental results show large scatter. Marreno and Mason (1972) suggested that the best experimental values for diffusivity of water vapor in air are those of O'Connell *et al.* (1969). In order to extrapolate the diffusivity of water vapor in air at temperatures below 0°C we have utilized the theory given by Mason and Monchick (1963) and the measurements of O'Connell *et al.* (1969). Although Mason's theory predicts dif-

fusivities which are low by a factor of about 10% when compared to most experimental results at temperatures above 0°C, we assume that the theory predicts at least the correct trend with temperature below 0°C. With this in mind we extrapolated the experimental results to predict values of the diffusivity of water vapor in air at temperatures below 0°C. The extrapolation method was suggested to us in a personal communication with Professor E. A. Mason (1975). Fitting an equation to the extrapolated data yielded

$$\mathfrak{D}[\mathrm{cm^2\ s^{-1}}]=0.211(T/T_0)^{1.94}(p_0/p) \qquad (13)$$

for the diffusivity of water vapor in air, applying to temperatures between −80 and 40°C, where $T_0=273.15$ K, and $P_0=1013.25$ mb.

b. Stationary diffusion shape factor

It has been customary (Mason, 1971; Fletcher, 1962; Byers, 1965) to follow Jeffreys (1918) and use an electrostatic analog for describing the field of water vapor around an arbitrary shaped ice particle growing or evaporating by diffusion of water vapor. This analogy depends upon two assumptions: 1) that the potential of the water vapor density, as does the electrostatic potential of a conductor, satisfies Laplace's equation, and 2) that it has a constant value at the surface and at infinity. In light of the recent relaxation time studies of Watts and Farkh (1975) the first assumption appears to be justifiable for ice particles of size typically present in cirrus clouds. The second approximation seems to be physically reasonable considering that the thermal conductivity of ice is about two orders of magnitude larger than that for air. Using the electrostatic analog, the shape effect of an ice particle on the diffusion of water vapor may then be expressed by the self capacitance C. Unfortunately, analytical expressions for this quantity are only available for simple geometrical shapes such as that of a sphere, an oblate and prolate spheroid, and a disk. However, experiments by McDonald (1963) and Podzimek (1966) indicated generally fair agreement between the capacitance for these simple shapes and geometrically more complex shapes which are observed for natural ice crystals. Some of the discrepancies found by these authors for specific shapes seem relatively small in comparison to the large scatter found in the observed characteristic dimensions of cirrus ice particles. We therefore used $C=r$ for a spherical ice particle, $C=LE/\ln[(1+E)/(1-E)]$ for a columnar shaped ice crystal, and $C=0.5\ dE/\sin^{-1}(E)$ for a plate-like ice crystal, where $E=[1-(\text{length along minor axis/length along major axis})^2]^{\frac{1}{2}}$.

c. Ventilation factors

Enhancement of mass diffusion caused by air motions around bodies from which diffusion takes place is frequently described in terms of a mean Sherwood number, $\bar{N}_{Sh}$. Alternatively, in meteorological literature this enhancement is often expressed in terms of a quantity called the ventilation coefficient f_m. These two quantities are related to each other by Eq. (2). Experimental evidence in the literature shows that the Sherwood number for bodies of various shapes can be correlated to the Schmidt number N_{Sc} and the Reynolds number N_{Re} by

$$\bar{N}_{Sh}=(\bar{N}_{Sh})_0+CN_{Sc}^m N_{Re}^n, \qquad (14)$$

where c, m, n are constants, and $(\bar{N}_{Sh})_0$ is the mean Sherwood number for a stationary particle for which $N_{Re}=0$.

Recent wind tunnel studies of the ventilation coefficient of spherical water drops in air carried out by Beard and Pruppacher (1971) showed that

$$\bar{N}_{Sh}=\begin{cases}2.00+0.216(N_{Sc}^{\frac{1}{3}}N_{Re}^{\frac{1}{2}})^2, & N_{Sc}^{\frac{1}{3}}N_{Re}^{\frac{1}{2}}<1.4\\ 1.56+0.616N_{Sc}^{\frac{1}{3}}N_{Re}^{\frac{1}{2}}, & N_{Sc}^{\frac{1}{3}}N_{Re}^{\frac{1}{2}}>1.4.\end{cases} \qquad (15)$$

Unfortunately, only few experiments have been carried out on the effect of ventilation on mass and heat transfer to bodies of shapes other than spherical. From a study of the heat and mass transfer rates involving 20 differently shaped particles including cylindrical shaped bodies, Pasternak and Gauvin (1960) found that at large Reynolds numbers the Sherwood number correlated well with the Reynolds number when the Reynolds number was based upon a characteristic length L^* defined as the ratio of the total surface area to the perimeter normal to the flow. (Note that hexagonal ice plates and ice columns in the atmosphere fall in such a way that their maximum dimension is oriented perpendicular to the direction of fall.) Unfortunately, Pasternak and Gauvin's values reported for the mean Sherwood number are not useful because the Reynolds numbers studied were much larger than encountered by cirrus ice particles. However, we still retained their method of data correlation and used L^* as a measure of the particle's exposed area in the flow field since it is this exposed area which controls the amount of enhancement to the diffusion process for a particular particle shape.

There exist only a few theoretical determinations of the ventilation coefficient for shapes other than spheres at intermediate Reynolds numbers. Among these are the numerical solutions by Masliyah and Epstein (1971, personal communication) who solved the convective diffusion equation for oblate spheroids of axis ratio 0.2, and by Pitter *et al.* (1974) who numerically solved the same equation for oblate spheroids of axis ratio 0.05.

To correlate available data for different shaped bodies presents a problem since the Sherwood number at zero Reynolds number $(\bar{N}_{Sh})_0$ depends on the shape of the crystal [see Eq. (3)]. However, this problem can be

circumvented by introducing the ventilation coefficient f_m for mass transfer defined by Eq. (2) which at zero Reynolds number is unity, independent of shape. Correlating the available data for a sphere and oblate spheroids of different axis ratios with the Reynolds number based upon the characteristic length L^* as suggested by Pasternak and Gauvin (1960), we arrived at a general expression for the ventilation coefficient f_m for mass transfer. This expression is

$$f_m=\begin{cases}1.00+0.14(N_{Sc}^{\frac{1}{3}}N_{Re,L^*}^{\frac{1}{2}})^2, & N_{Sc}^{\frac{1}{3}}N_{Re,L^*}^{\frac{1}{2}}<1.0\\ 0.86+0.28N_{Sc}^{\frac{1}{3}}N_{Re,L^*}^{\frac{1}{2}}, & N_{Sc}^{\frac{1}{3}}N_{Re,L^*}^{\frac{1}{2}}>1.0,\end{cases} \quad (16)$$

where in the atmosphere $N_{Sc}=(\eta/\rho_a\mathfrak{D})\approx 0.63$, where η is the dynamic viscosity of air (SMT). Values for f_m determined from this general formula deviate by less then 10% from the values for f_m for any specific shape when $N_{Sc}^{\frac{1}{3}}N_{Re}^{\frac{1}{2}}<10$, which is the range for typical cirrus ice particles.

Analogously, one may correlate the ventilation coefficient f_Q for thermal diffusion with available data by simply replacing the Schmidt number N_{Sc} by the Prandtl number N_{Pr}, yielding

$$f_Q=\begin{cases}1.00+0.14(N_{Pr}^{\frac{1}{3}}N_{Re,L^*}^{\frac{1}{2}})^2, & N_{Pr}^{\frac{1}{3}}N_{Re,L^*}^{\frac{1}{2}}<1.0\\ 0.86+0.28N_{Pr}^{\frac{1}{3}}N_{Re,L^*}^{\frac{1}{2}}, & N_{Pr}^{\frac{1}{3}}N_{Re,L^*}^{\frac{1}{2}}>1.0\end{cases} \quad (17)$$

where in the atmosphere $N_{Pr}=(\eta c_p/K)\approx 0.72$.

d. The evaporation coefficient for ice

β is defined as the ratio of the actual number of water molecules leaving the ice surface during evaporation to the number predicted by kinetic theory on the basis of the ice surface's equilibrium vapor pressure. A summary of the best experimentally derived values for the evaporation coefficient of ice has been given by Fukuta and Armstrong (1974). Their summary shows that the values scatter considerably between 1.0 and 0.01, a result which is probably due to the many experimental difficulties inherent in such a study. Some of these difficulties stem from problems in measuring the temperature of the ice surface and the water vapor pressure during non-steady-state conditions, while other difficulties arise from surface contamination during the experiment. In the present experiment, we therefore did not commit ourselves to one particular value of β, but rather determined the effect of a range of values on the survival distance of cirrus ice particles.

e. The thermal accommodation coefficient

The coefficient α is defined as the fraction of the air molecules which achieve thermal equilibrium while striking an ice surface. Unfortunately, only a few experimental estimates of this quantity are available. Strickland-Constable (1968) cites a value of 0.96. For lack of better information or contrary physical reasons, this study assumes $\alpha\approx 1$.

4. Results

a. Radiation effects

In the present problem heat transfer by radiation is due to the difference between the incoming radiation which is absorbed by the ice particle and the outgoing radiation emitted by the ice particle. Estimating this net flux is rather complex since it involves describing the absorption and emission properties of an ice particle in the radiation field of the earth's atmosphere. In order to get some feeling of the importance of this heat transfer process we determined how sensitive the evaporation rate is to a given net radiative heat flux Φ_R.

With the radiative heat flux prescribed, the problem was reduced to comparing the ice particle's surface temperature T_s with and without radiative heat transfer:

With radiative heat transfer

$$(T_s)_{\Phi_R}=T_\infty+\frac{S\Phi_R+\mathfrak{L}_s\left(\frac{dm}{dt}\right)_{\Phi_R}}{4\pi CF_\alpha Kf_Q}. \quad (18)$$

Without radiative heat transfer

$$(T_s)_{\Phi_R=0}=T_\infty+\frac{\mathfrak{L}_s\left(\frac{dm}{dt}\right)_{\Phi_R=0}}{4\pi CF_\alpha Kf_Q}. \quad (19)$$

Letting $T_s=(T_s)_{\Phi_R=0}$, combining Eqs. (18) and (19) and considering Eq. (1), one may express the surface temperature difference due to the net radiative heat flux Φ_R as

$$\Delta T_s=\frac{S\Phi_R}{4\pi C\left[F_\alpha Kf_Q+\mathfrak{L}_sF_\beta\mathfrak{D}\frac{\partial\rho_{sat,i}(T_s)}{\partial T}f_m\right]}. \quad (20)$$

In order to determine the effect of the computed temperature change ΔT_s on the evaporation rate, we introduced the relative humidity with respect to ice saturation

$$RH=\rho_{v,\infty}/\rho_{sat,i}(T_\infty). \quad (21)$$

From Eq. (1) the mass transfer rate with no radiative heat exchange can then be written as

$$\left(\frac{dm}{dt}\right)_{\Phi_R=0}=4\pi CF_\beta\mathfrak{D}[RH\rho_{sat,i}(T_\infty)-\rho_{sat,i}(T_s)]f_m. \quad (22)$$

Similarly, for the case when there is radiative heat exchange,

$$\left(\frac{dm}{dt}\right)_{\Phi_R}=4\pi CF_\beta\mathfrak{D}[RH\rho_{sat,i}(T_\infty)-\rho_{sat,i}(T_s+\Delta T)]f_m. \quad (23)$$

Assuming that we may set $\rho_{\text{sat},i}(T_s+\Delta T_s)=\rho_{\text{sat},i}(T_s)+[\partial\rho_{\text{sat},i}(T_s)/\partial T]\Delta T_s$, and defining the effective radiative relative humidity as

$$\text{RH}^*=\text{RH}-\frac{1}{\rho_{\text{sat},i}(T_\infty)}\left[\frac{\partial\rho_{\text{sat},i}(T_s)}{\partial T}\right]\Delta T_s, \quad (24)$$

we obtained analogous to Eq. (22) for the mass transfer with radiative heat transfer

$$\left(\frac{dm}{dt}\right)_{\Phi_R}=4\pi CF_\beta\mathfrak{D}[\text{RH}^*\rho_{\text{sat},i}(T_\infty)-\rho_{\text{sat},i}(T_s)]f_m. \quad (25)$$

In order to evaluate Eq. (24) we needed to specify values for Φ_R which allowed us to determine ΔT_s from Eq. (20).

The net radiative heat flux Φ_R is equal to the difference between the amount of impinging radiation Φ_I upon the ice particle's surface which is absorbed by the ice particle, and the radiation that is emitted by the particle's surface, i.e.,

$$\Phi_R=\Phi_I(1-\overline{R(\lambda)})\overline{A(\lambda)}-\epsilon\sigma T_s^4, \quad (26)$$

where $\overline{R(\lambda)}$ is the reflectivity, $\overline{A(\lambda)}$ the absorptivity of the ice particle and ϵ the emissivity of ice.

The spectrally weighted reflectivity and absorptivity can be written as

$$\overline{R(\lambda)}=\frac{1}{\sigma T^4}\int_0^\infty B(T,\lambda)R(\lambda)d\lambda, \quad (27)$$

$$\overline{A(\lambda)}=\frac{1}{\sigma T^4}\int_0^\infty B(T,\lambda)A(\lambda)d\lambda, \quad (28)$$

where $B(T,\lambda)$ is the Planck spectrum function. For a ray impinging normal to a surface the reflectivity is

$$R(\lambda)=\frac{(n_r-1)^2+n_i^2}{(n_r+1)^2+n_i^2}. \quad (29)$$

The absorptivity is

$$A(\lambda)=1-\exp\left(-\frac{4\pi n_i}{\lambda}s\right). \quad (30)$$

In Eqs. (29) and (30) n_r and n_i are the real and imaginary parts of the refractive index of ice as given by Irvine and Pollack (1968), and s is the distance in centimeters the impinging ray traverses through the ice particle. Evaluating Eqs. (27) and (28) we found $\overline{R(\lambda)}=0.034$, and $\overline{A(\lambda)}=1-\exp(-87.0\,s^{0.77})$ insensitive to temperatures between -10 and -50°C.

Unfortunately, the emissivity of ice ϵ has not been measured at cirrus cloud temperatures. We therefore could only make an estimate of this quantity. Using the results of Dunkle *et al.* (1957) we assumed for the infrared emissivity of ice $\epsilon=0.9\pm0.1$.

Valovcin (1968) and Kuhn and Weickmann (1969) found that at cirrus cloud levels the impinging radiation onto an ice particle surface is highly variable, depending predominantly on cloudiness. We therefore decided to propose physical limits for Φ_I.

For the case of *maximum warming* we assumed that Φ_I can be expressed as

$$\Phi_I=\tfrac{1}{2}[\sigma(T_{\text{ground}}+T_s^4)]. \quad (31)$$

Eq. (31) assumes that the radiation emitted by the ground impinges directly on the cirrus ice particle surface without attenuation in the atmosphere and further that the radiation received by the ice particles from above has a blackbody temperature equal to the temperature of the ice particle.

For the case of *maximum cooling* we assumed that Φ_I can be expressed as

$$\Phi_I=\tfrac{1}{2}\sigma T_s^4 \quad (32)$$

Eq. (32) assumes that the condition where the radiation emitted by the ground is completely attenuated by clouds on the way to the cirrus ice particle, that the minimum upward radiation flux has a blackbody temperature equal to the temperature of the ice particle, and that the corresponding downward radiation flux from above to the ice particle is zero. The observations of Valovcin (1968) and Kuhn and Weickmann (1969) fall well within these proposed limits.

Tables 1–3 express the sensitivity of the evaporation rate of cirrus ice particles of various shapes and sizes to radiative heat transfer in terms of an effective change in relative humidity (with respect to ice saturation),

TABLE 1. Effective relative humidity change (percent) due to radiative heat exchange for a spherical ice particle falling in the NASA Standard Atmosphere at different levels.

		Cooling case			
		Radius (μm)			
P (mb)	T (°C)	40	80	120	160
200	−56.6	1.86	2.90	3.46	3.86
300	−44.6	1.90	2.88	3.40	3.77
400	−31.7	1.84	2.75	3.22	3.56
500	−21.3	1.68	2.46	2.87	3.17
		Warming case*			
		Radius (μm)			
P (mb)	T (°C)	40	80	120	160
200	−56.6	−1.98	−4.77	−6.32	−7.29
300	−44.6	−1.26	−3.26	−4.35	−5.02
400	−31.7	−0.63	−1.96	−2.69	−3.12
500	−21.3	−0.22	−1.11	−1.58	−1.86

* $T_{\text{ground}}=15$°C.

TABLE 2. Effective relative humidity change (percent) due to radiative heat exchange for a columnar ice particle falling in the NACA Standard Atmosphere at different levels.

		Cooling case			
		Length (μm)			
P (mb)	T (°C)	400	600	800	1000
200	−56.6	3.33	4.00	4.54	5.00
300	−44.6	3.33	3.98	4.50	4.90
400	−31.7	3.19	3.80	4.29	4.71
500	−21.3	2.87	3.41	3.85	4.22
		Warming case*			
		Length (μm)			
P (mb)	T (°C)	400	600	800	1000
200	−56.6	−5.32	−6.93	−8.17	−9.20
300	−44.6	−3.66	−4.80	−5.68	−6.40
400	−31.7	−2.94	−2.94	−3.52	−3.98
500	−21.3	−1.22	−1.71	−2.07	−2.36

* $T_{\text{ground}}=15$°C.

defined by $\Delta RH^*=RH^*-RH$. The results are tabulated for the assumed maximum cooling case with $\epsilon=1.0$, and the assumed maximum warming case with $\epsilon=0.8$, and for various levels in the NACA Standard Atmosphere.

It is seen that the radiative heat transfer between cirrus ice particles in clear air and the earth-atmosphere radiation field can only change the effective relative humidity by a few percent. For the warming case the results predict that ΔRH^* increases with altitude due to the ice particle being at a colder temperature and further out of radiation equilibrium with the ground. The cooling case ΔRH^* appears to be rather constant with height. The results also show that ΔRH^* is sensitive to ice particle size and shape; ΔRH^* increases with size and is larger for a plate than a column, and larger for a column than a sphere of the same mass. The size and shape effects are not surprising considering the surface area differences of these ice particles. In order to see what effect these relative humidity changes have on the survival distance of cirrus ice particles, we integrated the mass transfer equation and simultaneously solved for the ice particle's trajectory and survival distance.

TABLE 3. Effective relative humidity change (percent) due to radiative heat exchange for a plate-like ice particle falling in the NACA Standard Atmosphere at different levels.

		Cooling case			
		Diameter (μm)			
P (mb)	T (°C)	400	600	800	1000
200	−56.6	5.74	7.27	8.51	9.55
300	−44.6	5.75	7.24	8.42	9.41
400	−31.7	5.51	6.90	8.02	7.99
		Warming case*			
		Diameter (μm)			
P (mb)	T (°C)	400	600	800	1000
200	−56.6	−5.93	−8.97	−11.61	−13.9
300	−44.6	−3.69	−5.82	−7.66	−9.26
400	−31.7	−1.76	−3.11	−4.30	−5.33
500	−21.6	−0.58	−1.41	−2.14	−2.79

* $T_{\text{ground}}=15$°C.

To perform this integration we first prescribed the temperature and humidity conditions in the atmosphere. These determined T_∞, $\rho_{v,\infty}$. This then allowed computing the mass change in time of a falling ice particle by simultaneously solving Eqs. (1)–(12) together with Eq. (26). Specifying the trajectory of the ice particle further required knowledge of the particles' terminal velocity which depends on the mass, shape and height of the particle. Neglecting vertical air motions in the surroundings of the falling ice particle, the change in height z of the ice particle with respect to time t was assumed to be given by

$$\frac{dz}{dt}=-V_\infty, \tag{33}$$

where V_∞ is the terminal fall velocity of the ice particle. To express the terminal velocity of a spherical ice particle we utilized the relationships given by Beard (1976), while for columnar and plate-like ice particles we utilized the relationships given by Jayaweera and Cottis (1969) together with the interpolation formula for ice columns given by Heymsfield (1972). In order to describe the change in shape caused by a change in mass, we used the field observations of Heymsfield and Knollenberg (1972) to describe the dimensional relation for columnar ice particles in cirrus clouds, and the field observations of Auer and Veal (1970) to describe the dimensional relation for simple hexagonal

TABLE 4. Calculated fall distances for a columnar ice particle at various relative humidities in the NACA Standard Atmosphere with and without radiative heat exchange. Initial size, 164×800 μm; initial height of ice particle, 9.15×10^3 m; ice particle bulk density, 0.7×10^{-3} kg m^{-3}. Case 1, no radiative heat exchange; case 2, proposed maximum cooling conditions; case 3, proposed maximum heating conditions.

	Case 1		Case 2		Case 3	
RH (percent)	Final height (km)	Surviving distance (km)	Final height (km)	Surviving distance (km)	Final height (km)	Surviving distance (km)
30	8.02	1.13	7.96	1.20	8.07	1.08
50	7.73	1.42	7.63	1.52	7.82	1.33
70	7.20	1.95	7.00	2.15	7.37	1.78
90	5.61	3.54	4.73	4.42	6.31	2.85

plates. These authors describe various ice particle shapes by two characteristic dimensions (i.e., length vs thickness or diameter vs height) in the general form of $L_1=g_1(L_2)$. In our computations we assumed that an ice particle retains the dimensional relationship observed during diffusional growth, as well as during diffusional evaporation.

Given the characteristic dimensions of an ice particle and its bulk density, the equation describing the ice particle mass has the functional form of $m=g_2(L_1,L_2,\rho_s)$. Thus the equations describing the change in the two characteristic lengths are

$$\frac{dL_2}{dt}=\frac{dm/dt}{\left(\frac{\partial g_2}{\partial L_1}\frac{dg_1}{dL_2}+\frac{\partial g_2}{\partial L_2}\right)}, \tag{34}$$

$$\frac{dL_1}{dt}=\frac{dg_1}{dL_2}\frac{dL_2}{dt}, \tag{35}$$

where for columnar ice particles of cirrus clouds, with $L_1=w$ and $L_2=L$, Heymsfield and Knollenberg (1972) suggested

$$w[\text{cm}]=0.0627L^{0.53}, \tag{36}$$

and for simple hexagonal ice plates with $L_1=h$ and $L_2=d$, Auer and Veal (1970) suggested

$$h[\text{cm}]=0.01263d^{0.449}. \tag{37}$$

In order to numerically solve the system of differential equations which describe the change in mass, length, width and height of the ice particle, we used Hamming's modified predictor-corrector method. An ice particle was followed on its trajectory until a level in the atmosphere was reached where the maximum dimension of the ice particle became less than 20 μm, i.e., where its terminal velocity is sufficiently small that the remaining particle mass evaporated at that level. The results of such calculations are displayed in Table 4 which shows the effect of radiative heat exchange on the fall distance of columnar ice particles in the NACA Standard Atmosphere of various relative humidities. We see that the survival distance of such ice particles is shortened by the assumed maximum warming rate and lengthened by the assumed maximum cooling rate by less than 10% if the ambient relative humidity is less than 70%. At larger relative humidities the radiative effects can become significant when considering these assumed limits. Note, however, that the assumed limits are probably not applicable at high humidities when the atmosphere is most likely cloudy. In a cloudy atmosphere an ice particle will be in radiative equilibrium with its close surroundings and thus have little radiative heat exchange. From our sensitivity analysis we drew the conclusion that radiative heat transfer to and from a cirrus ice particle is only of secondary importance in determining its survival distance in subsaturated air. In the study which now follows the radiative heat transfer effects were therefore ignored.

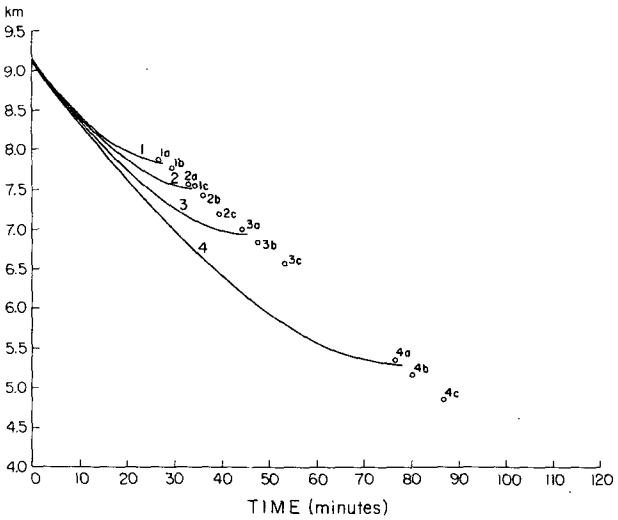

FIG. 1. Theoretically computed fall distance for a spherical ice particle falling in subsaturated air as a function of relative humidity and evaporation coefficient (NACA Standard Atmosphere). Initial mass of ice particle, 1.2×10^{-8} kg; $\rho_s=0.7\times10^{-3}$ kg m^{-3}; initial ice particle radius, 160 μm.

(1) Relative humidity=30% for $\beta=0.1$
(2) Relative humidity=50% for $\beta=0.1$
(3) Relative humidity=70% for $\beta=0.1$
(4) Relative humidity=90% for $\beta=0.1$. (1a), (2a), (3a), (4a): corresponding end locations for $\beta=1.0$; (1b), (2b), (3b), (4b): corresponding end locations for $\beta=0.03$; (1c), (2c), (3c), (4c): corresponding end locations for $\beta=0.01$.

b. *Kinetic effects*

In order to determine the effect of the evaporation coefficient on the survival distance of cirrus ice particles,

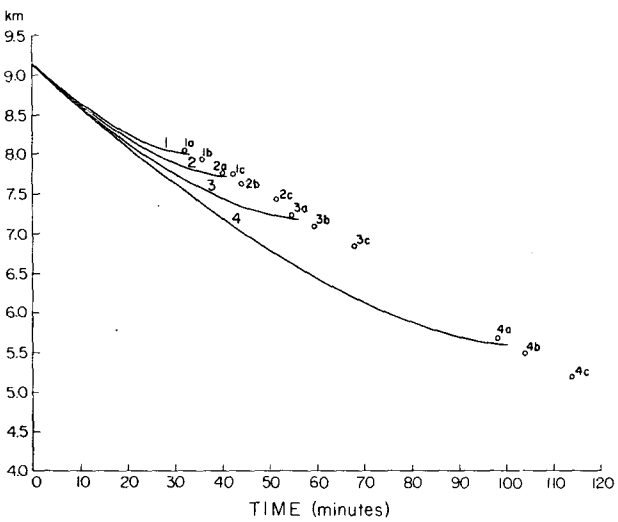

FIG. 2. As in Fig. 1 except for a columnar ice particle. Initial length×width: 800 μm×164 μm.

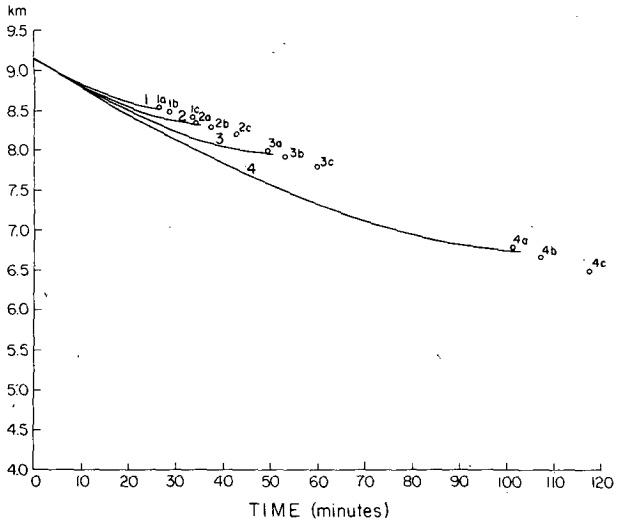

FIG. 3. As in Fig. 1 except for a plate-like ice particle. Initial diameter×thickness: 800 μm×41 μm.

we solved the above described set of equations for the case of various values of β. The results of these computations are displayed in Figs. 1–3. Comparing these three figures one sees that a spherical ice particle falls farther than a columnar ice particle and that the columnar ice particle farther than a plate-like ice particle. Also, it is seen that as β decreases, the survival distance of an ice particle is lengthened. However, this lengthening is typically less than 0.5 km and independent of the relative humidity of the ambient air.

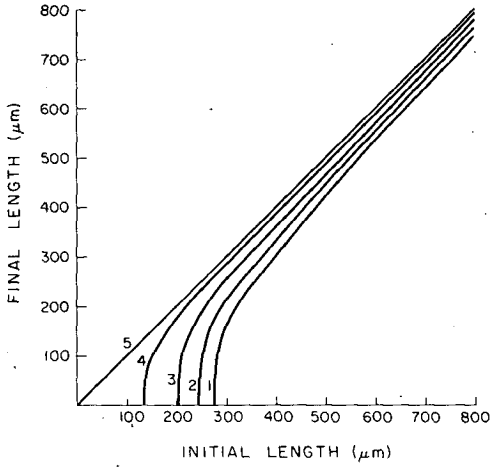

FIG. 4. Initial vs final size of a columnar ice particle after falling 200 m in ice-subsaturated air of $p=300$ mb and $T=-44.9$°C for various relative humidities (NACA Standard Atmosphere).

(1) Relative humidity=30% for $\beta=0.1$
(2) Relative humidity=50% for $\beta=0.1$
(3) Relative humidity=70% for $\beta=0.1$
(4) Relative humidity=90% for $\beta=0.1$
(5) Limiting case of no evaporation.

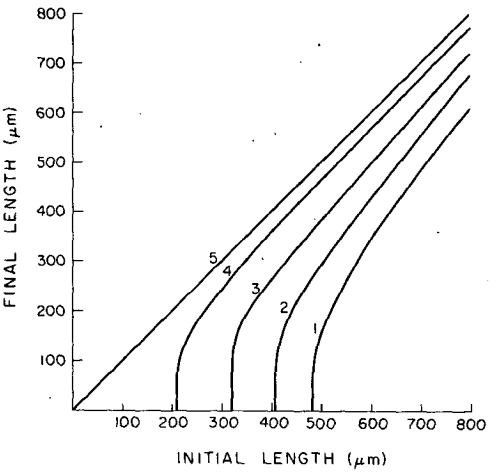

FIG. 5. As in Fig. 4 except for $p=400$ mb and $T=-32.7$°C.

c. *Size effect*

In order to illustrate the effect of the size of cirrus ice particles on their survival distance we chose to compute the initial vs the final size of a columnar ice particle falling at given pressure, temperature and humidity of the ambient air over a distance of 200 m. The results of these computations are summarized in Figs. 4–7. Considering first the effect of humidity, we notice from Fig. 4 that if a particle is larger than about 400 μm it can survive a 200 m fall without significant change in size with little dependence on humidity if the temperature is below −40°C. For temperatures warmer than −40°C the effect of humidity on the survival characteristics of cirrus ice particles becomes increasingly important (see Figs. 5–7). Figs. 4–7 demonstrate further that at any given temperature and pressure an ice particle must be larger than a critical size to survive a fall of 200 m. For instance, at 90% relative humidity the critical length of a columnar crystal is about 135 μm at −44.9°C and 300 mb, 210 μm at −32.7°C and

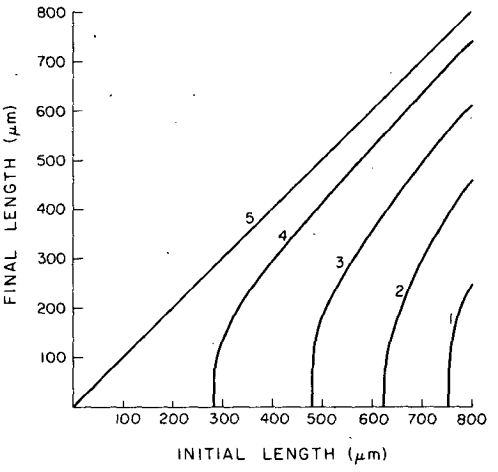

FIG. 6. As in Fig. 4 except for $p=500$ mb and $T=-21.7$°C.

400 mb, 280 μm at -21.7°C and 500 mb, and 370 μm at -12.4°C and 600 mb.

d. Comparison with two field observations

Much of the motivation for this work came from the observations of Braham and Spyers-Duran (1967) whose results shall now be discussed in the light of the present computations. Flying beneath cirrus clouds, these authors noted that cirrus ice particles survived a fall distance of up to 5 km in very low humidity conditions. The results displayed in Fig. 8 are derived from our computations for one of their cases. The right side of Fig. 8 shows the temperature and dew point structure of the atmosphere, the altitude of the cirrus, and collection level of the observer's aircraft over Bemidji, Minn., on 8 July 1966. We chose to make computations for this particular case because there were no lower level clouds observed, thus eliminating the possibility that the observed ice particles might have come from somewhere other than the cirrus above. The concentration of the ice particles found ranged from 10^2 to 10^3 per cubic liter at a distance of 5 km below the cirrus. The left side of Fig. 8 gives the results of our calculations for a spherical and a columnar ice particle of various bulk densities but the same initial size corresponding to typical larger cirrus ice particles. The initial height of the ice particle was 9.16 km (300 mb) and the ice particles were allowed to fall at their own terminal velocity. The results show that under such conditions a typical large cirrus ice particle will only survive a distance of 1–1.5 km. This distance is considerably shorter than the 5 km reported. Curve 4 shows that an ice particle would have had to be of spherical shape and of an initial radius of 350 μm in order to have survived the reported distance. The ice particle mass corresponding to such a particle seems unrealistic for cirrus cloud particles. The most likely reason for the discrepancy between the calculations

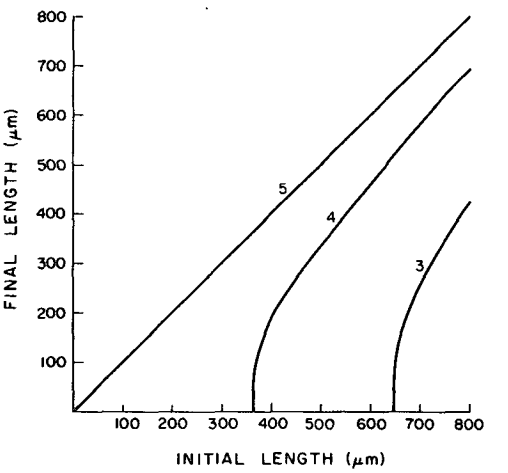

FIG. 7. As in Fig. 4 except for $p=600$ mb and $T=-12.4$°C.

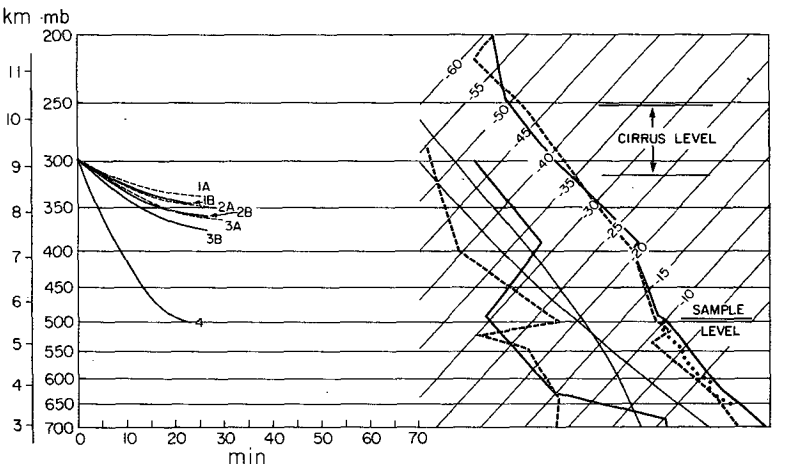

FIG. 8. Observational data and theoretical results for Braham and Spyers-Duran (1967) case. Right: temperature and moisture structure of atmosphere on 8 July 1966, given by Braham and Spyers-Duran. Solid lines, temperature and dew point (RAOB, International Falls, 90 mi northeast of site); dashed lines, temperature and dew point (RAOB, Bismark, 290 mi west of site); dotted line, aircraft temperature at site. Left: theoretical computed results for columnar and spherical ice particles of various densities falling from observed cirrus cloud base.

(1) $\rho_s=0.6\times10^{-3}$ kg m^{-3}, $\beta=0.0144$; (A) column, 800×164 μm; (B) sphere, $r_0=160$ μm

(2) $\rho_s=0.75\times10^{-3}$ kg m^{-3}, $\beta=0.0144$; (A) column, 800×164 μm; (B) sphere, $r_0=160$ μm

(3) $\rho_s=0.9\times10^{-3}$ kg m^{-3}, $\beta=0.0144$; (A) column, 800×164 μm, (B) sphere, $r_0=160$ μm

(4) $\rho_s=0.9\times10^{-3}$ kg m^{-3}, $\beta=0.0144$, sphere, $r_0=350$ μm.

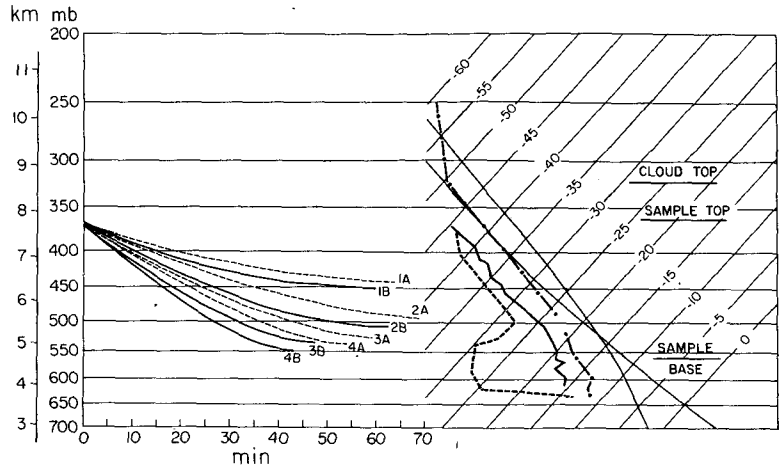

FIG. 9. As in Fig. 8 except for Heymsfield (1973) case. Right: temperature and moisture structure of the atmosphere on 4 March 1972, given by Heymsfield. Dot-dashed line, temperature (ROAB, Salem, Ill., at same location and time as aircraft cloud study); solid line, aircraft temperature measured during observation. Left: theoretical computed results for columnar and spherical ice particles of various densities falling from observed cirrus cloud base.

(1) $\rho_s=0.3\times10^{-3}$ kg m^{-3}, $\beta=0.144$, (A) column, initial size, 800×164 μm, (B) sphere, initial radius, 160 μm

(2) $\rho_s=0.5\times10^{-3}$ kg m^{-3}, $\beta=0.0144$, (A) column, initial size, 800×164 μm, (B) sphere, initial radius, 160 μm

(3) $\rho_s=0.75\times10^{-3}$ kg m^{-3}, $\beta=0.0144$, (A) column, initial size, 800×164 μm, (B) sphere, initial radius, 160 μm

(4) $\rho_s=0.90\times10^{-3}$ kg m^{-3}, $\beta=0.0144$, (A) column, initial size, 800×164 μm, (B) sphere, initial radius, 160 μm.

and the observation is that the humidity conditions reported from weather stations 90 and 290 mi away from the observation site do not accurately reflect the humidity conditions directly along the paths of the falling cirrus ice particles. Such a possibility was already envisioned by Braham and Spyers-Duran (1967).

This explanation becomes more credible if we consider the field observations of Heymsfield (1973) who studied evaporating cirrus ice particles in and below a cirrostratus cloud over Salem, Ill., on 4 March 1972, where simultaneous temperature and humidity data were available. Fig. 9 summarizes the observations and computations for this case. The right side of Fig. 9 shows the temperature and dew point distribution reported by the Salem weather station for the same location time at which the flight was carried out. Also, on the right are plotted the cloud top and region beneath the cirrostratus deck where ice particles were observed by the aircraft. The line marked "sample base" corresponds to the lowest level at which the cirrus ice particles were detected. The left side of Fig. 9 presents the results of our calculations for columnar and spherical ice particles of various densities. We see that our theoretically predicted survival distances of cirrus ice particles are in good agreement with those observed by Heymsfield (1973).

Unfortunately, no other well-documented flights in and beneath cirrus clouds have been reported in the literature. In the light of this fact we express the hope that more observations will become available in the near future which would make it possible to substantiate the present tentative conclusion that high relative humidities are required for cirrus ice particles to survive the considerable fall distances needed in order to "seed" supercooled clouds at lower levels. Such observations would also be of importance in helping to further substantiate the validity of the equations describing the diffusional growth and evaporation of ice particles.

Acknowledgments. The authors are indebted to the National Science Foundation for providing funds under Grant DES 75-09999 which were used to carry out the present work. They would also like to acknowledge the fruitful discussions with Dr. A. Heymsfield on the interpretation of cirrus microphysical data, and the guidance provided by Dr. S. V. Venkateswaran in formulating an estimate for the radiative heat transfer effects on cirrus ice particle evaporation.

APPENDIX

List of Symbols

$A(\lambda)$	absorptivity for radiation
$\overline{A(\lambda)}$	spectral weighted absorptivity
$B(T,\lambda)$	Planck spectral function

C electrostatic self capacitance of a conductor with the same shape and size as the ice particle
c_p specific heat of moist air at constant pressure
d diameter of a plate like ice particle
$\mathfrak{D}$ diffusivity of water vapor in air
f_m ventilation coefficient for mass diffusion
f_Q ventilation coefficient for heat diffusion
F_α kinetic correction factor to the heat diffusion equation
F_β kinetic correction factor to the mass diffusion equation
$g_1(L_2)$ functional form describing an ice particle shape
h thickness of plate like ice particle
K thermal conductivity of moist air $\{=K_d[1-(1.17-1.02\ K_vK_d^{-1})\rho_v\rho_a^{-1}]$, where K_d[cal cm^{-1} s^{-1} °C^{-1}] $=(5.69+0.168\ T)\times10^{-5}$, K_v[cal cm^{-1} s^{-1} °C^{-1}] $=(3.73+0.020\ T)\times10^{-5}$, with T in °C$\}$
L length of columnar ice particle
l_m^* as defined by Eq. (6)
l_Q^* as defined by Eq. (9)
L_1, L_2 characteristic dimensions of an ice particle
L^* characteristic length defined as the total surface area divided by the perimeter normal to the flow for the ice particle
$\mathfrak{L}_s$ latent heat of sublimation for ice
m mass of ice particle
M_w molecular weight of water
n_i imaginary part of the index of refraction of ice
n_r real part of the index of refraction of ice
$\bar{N}_{Nu}$ mean Nussett number
$(\bar{N}_{Nu})_0$ Nussett number for a stationary ice particle
N_{Pr} Prandtl number[$=\eta c_p/K$]
N_{Re} Reynolds number
N_{Re,L^*} Reynolds number based on L^*
N_{Sc} Schmidt number[$=\eta/\rho_a\mathfrak{D}$]
$(\bar{N}_{Sh})_0$ mean Sherwood number for the stationary ice particle
$\bar{N}_{Sh}$ mean Sherwood number
p total atmospheric pressure
p_0 1013.25 mb
P perimeter of ice particle normal to flow
Q heat
r radius of spherical ice particle
r^* as defined by Eq. (5)
$\mathfrak{R}$ universal gas constant
R_d specific gas constant for dry air
RH relative humidity with respect to ice saturation
RH* effective relative humidity with respect to ice saturation due to radiative heat transfer
$R(\lambda)$ reflectivity for radiation
$\overline{R(\lambda)}$ spectral weighted reflectivity
s absorbing distance of ray traveling through the ice particle
S total surface area of ice particle
t time
T absolute temperature
T_{ground} temperature of ground
T_0 273.15°K
T_s temperature at ice particle's surface
T_∞ environmental temperature
$\bar{v}_r$ average velocity of the air molecules striking the ice particle's surface [$=(8R_dT_s/\pi)^{\frac{1}{2}}$]
V_∞ terminal velocity of the ice particle
w width of columnar ice particle
z height
α thermal accommodation coefficient
β evaporation coefficient
ΔRH* effective relative humidity change with respect to ice due to radiative heat transfer
ΔT_s temperature change of ice particle due to radiative heat transfer
ϵ emissivity of ice
E eccentricity of oblate or prolate spheroid
η dynamic viscosity of air [$=1.8325\times10^{-4}(T/296.16)^{1.5}(T+120)/(T+296.16)$, with T in °K]
λ wavelength of radiation
Φ_I impinging flux of radiation upon the ice particle
Φ_R net radiative heat flux to ice particle
ρ_a density of air
ρ_s ice particle bulk density
$\rho_{sat,i}(T)$ saturated vapor density at temperature T with respect to ice
$\rho_{v,\infty}$ environmental water vapor density
σ Stefan-Boltzman constant

REFERENCES

Auer, Jr., A. H., and D. L. Veal, 1970: The dimension of ice crystals in natural clouds. *J. Atmos. Sci.*, **27**, 919–926.

Beard, K. V., 1976: Terminal velocity and shape of cloud and precipitation drops. *J. Atmos. Sci.*, **33**, 851–864.

——, and H. R. Pruppacher, 1971: A wind tunnel investigation of the rate of evaporation of small water drops falling a terminal velocity in air. *J. Atmos. Sci.*, **28**, 1455–1464.

Braham, R. R., 1967: Cirrus cloud seeding as a trigger for storm development. *J. Atmos. Sci.*, **24**, 311–312.

——, and P. Spyers-Duran, 1967: Survival of cirrus crystals in clear air. *J. Appl. Meteor.*, **6**, 1053–1061.

Byers, H. R., 1965: *Elements of Cloud Physics*. University of Chicago Press, 191 pp.

Dunkle, R. V., J. T. Gier and J. T. Bevans, 1957: Emissivity of ice, snow and frozen ground. *Refrig. Eng.*, **65**, 33–35.

Fitzgerald, J. W., 1974: Effect of aerosol composition on cloud droplet size distribution: A numerical study. *J. Atmos. Sci.*, **31**, 1358–1367.

Fletcher, N. H., 1962: *The Physics of Rain Clouds*. Cambridge University Press, 386 pp.

Fleming, J. R. and S. K. Cox, 1974: Radiative effects of cirrus clouds. *J. Atmos. Sci.*, **31**, 2182–2188.

Fuchs, N. A., 1959: *Evaporation and Droplet Growth in Gaseous Media*. Pergamon Press, 87 pp.

Fukuta, N., 1969: Experimental studies on the growth of small ice crystals. *J. Atmos. Sci.*, **28**, 728–736.

——, and J. A. Armstrong, 1974: Experimental determination of the deposition coefficient of water vapor onto ice. *Preprints Cloud Physics Conf.*, Tucson, Amer. Meteor. Soc., 46–49.

——, and L. A. Walter, 1970: Kinetics of hydrometeor growth from a vapor spherical model. *J. Atmos. Sci.*, **27**, 1160–1172.

Hall, W. D., 1976: The survival of cirrus ice particles falling beneath cirrus clouds in subsaturated air. Ph.D. thesis, University of California, Los Angeles, 170 pp.

Hansen, J. E., and J. B. Pollack, 1970: Near-infrared light scattering by terrestrial clouds. *J. Atmos. Sci.*, **27**, 265–281.

Heymsfield, A. J., 1972: Ice crystal terminal velocities. *J. Atmos. Sci.*, **26**, 1348–1351.

——, 1973: Cirrus uncinus generating cells and the evolution of cirriform clouds. Ph.D. thesis, University of Chicago, 269 pp.

——, 1975: Cirrus uncinus generating cells and the evolution of cirriform clouds: Parts I, II and III. *J. Atmos. Sci.*, **32**, 799–830.

——, and R. E. Knollenberg, 1972: Properties of cirrus generating cells. *J. Atmos. Sci.*, **21**, 1358–1366.

Hobbs, P. V., 1974: *Ice Physics*. Oxford University Press, 837 pp.

Irvine, W. M., and J. B. Pollack, 1968: Infrared optical properties of water and ice spheres. *Icarus*, **8**, 324–360.

Jayaweera, K. O. L. F., 1971: Calculations of ice crystal growth. *J. Atmos. Sci.*, **28**, 728–736.

——, and R. E. Cottis, 1969: Fall velocities of plate-like and columnar ice crystals. *Quart. J. Roy. Meteor. Soc.*, **95**, 703–709.

Jeffreys, H., 1918: Some problems of evaporation. *Phil. Mag.*, **35**, 270–280.

Jiusto, J. E., and H. K. Weickmann, 1973: Types of snowfall. *Bull. Amer. Meteor. Soc.*, **54**, 1148–1162.

Koenig, L. R., 1971: Numerical modeling of deposition. *J. Atmos. Sci.*, **28**, 226–237.

Kuhn, P. M., and H. K. Weickmann, 1969: High altitude radiometric measurements of cirrus. *J. Appl. Meteor.*, **8**, 147–154.

List, R. J., 1947: *Smithsonian Meteorological Tables*, 6th rev. ed. Smithsonian Institution Press, Washington, D. C.

Liou, K-N., 1973: Transfer of solar irradiance through cirrus cloud layers. *J. Geophys. Res.*, **78**, 1409–1418.

Marreno, T. R., and E. A. Mason, 1972: Gaseous diffusion coefficients. *J. Phys. Chem. Ref. Data*, **1**, 1–118.

Mason, B. J., 1971: *The Physics of Clouds*, 2nd ed. Oxford University Press, 671 pp.

Mason, E. A., and L. Monchick, 1963: Transport properties of polar-gas mixtures. *J. Chem. Phys.*, **36**, 2746–2757.

McDonald, J. E., 1963: The use of the electrostatic analogy in studies of ice crystal growth. *J. Appl. Math. Phys.*, **14**, 610–620.

O'Connell, J. P., M. D. Gillespie, W. D. Krostek and J. M. Prausnitz, 1969: Diffusivities of water in nonpolar gases. *J. Phys. Chem.*, **73**, 2000–2004.

Pasternak, I. S., and W. H. Gauvin, 1960: Turbulent heat and mass transfer from stationary particles. *Can. J. Chem. Eng.*, **38**, 35–42.

Pitter, R. L., H. R. Pruppacher and A. E. Hamielec, 1974: A numerical study of the effect of forced convection on mass transport from a thin oblate spheroid of ice in air. *J. Atmos. Sci.*, **31**, 1058–1066.

Platt, C. M., 1975: Infrared emissivity of cirrus—simultaneous satellite, lidar and radiometric observations. *Quart. J. Roy. Meteor. Soc.*, **101**, 119–126.

Podzimek, J., 1966: Experimental determination of the capacity of ice crystals. *Stud. Geophys. Geod.*, **10**, 235–238.

Schrage, R. W., 1953: *A Theoretical Study of the Interphase Mass Transfer*. Columbia University Press, 103 pp.

Strickland-Constable, R. F., 1968: *Kinetics and Mechanism of Crystallization*. Academic Press, 347 pp.

Valovcin, F. R., 1968: Infrared measurements of jet-stream cirrus. *J. Appl. Meteor.*, **7**, 817–826.

Watts, R. G., and I. Farkh, 1975: Relaxation times for stationary, evaporating liquid droplets. *J. Atmos. Sci.*, **32**, 1864–1867.

Weickmann, H. K., 1945: Formen und Bildung atmosphärischer Eiskristalle. *Beit. Phys. Atmos.*, **28**, 12–52.

——, 1949; Die Eisphase in der atmosphäre. *Ber. Deut. Wetterdienst*, No. 6, 54 pp.